Ionization cross sections of small cationic carbon clusters in high-energy collisions with helium atoms and stability of multiply charged species

F. Mezdari,[1] K. Wohrer-Béroff,[1] M. Chabot,[2] G. Martinet,[2] S. Della Negrâ,[2] P. Désesquelles,[2] H. Hamrita,[2] and A. LePadellec[3]

[1]*Laboratoire des Collisions Atomiques et Moléculaires (LCAM, UMR Université Paris Sud et CNRS, No. 8625), Bâtiment 351, Université Paris Sud, F-91405 Orsay, Cedex, France*

[2]*Institut de Physique Nucléaire, IN2P3-CNRS, F-91406 Orsay Cedex, France*

[3]*Laboratoire des Collisions Agrégats- Réactivité (LCAR, UMR Université Paul Sabatier et CNRS, No. 5589), Bâtiment III R1 B4, Université Paul Sabatier-Toulouse III, 118, Route de Narbonne, 31062 Toulouse Cedex 4, France*

(Received 3 February 2005; published 9 September 2005)

Single, double, triple, and quadruple ionization cross sections of small cationic carbon clusters C_n^+ colliding with helium atoms at a fixed velocity (2.6 atomic units) have been measured. The size ranges from $n=1$ to $n=10$ for single to triple ionization, from $n=5$ to $n=10$ for the quadruple ionization. The dependence of the cross sections with the cluster size is found to be well reproduced by predictions of the independent atom and electron (IAE) collision model. This extends the applicability of this simple model to higher n values and to a higher ionization degree than previously done [M. Chabot *et al.*, Eur. Phys. J. D **14**, 5 (2001)]. The branching ratios of multiply charged C_n^{q+} clusters remaining intact over a 100 ns time window have been measured ($n=3-10$, $q=2-3$). Branching ratios of nonfragmented doubly charged clusters have been interpreted on the basis of calculated internal energies of C_n^{2+} due to single ionization of C_n^+ clusters using the IAE model. This allowed estimates of the minimum energies required to fragment these C_n^{2+} species to be derived.

DOI: 10.1103/PhysRevA.72.032707 PACS number(s): 34.50.Gb, 36.40.Qv

I. INTRODUCTION

Small carbon clusters have been detected in the interstellar and circumstellar medium [1] as well as in comets [2]. These species and other present molecules are submitted to continuous [3] as well as sporadic particle bombardment (supernovae explosions for instance [4]) whose effect on the evolution of their populations could be of importance, especially in dense media not reached by the competing UV radiation [5]. The interaction of ions or atoms with clusters became an active field of research in the last decade. Experiments were performed in the domain of low velocity collisions ($v_p \ll 1$ a.u.), where vibrational excitation of the cluster prevails [6–9], as well as in the domain of high velocity ($v_p \gg 1$ a.u.) [10,11] and intermediate velocity ($v_p \sim 1$ a.u.) [12–15] collisions, where electronic excitation (mainly ionization) dominates. In the latter situation, which covers the present work, it has been shown that multiple ionization processes are large compared with single ionization cross sections, leading to the formation of multiply charged clusters. The stability of the formed species, which governs the destruction or nondestruction of the cluster, is an important issue. Experimental information on the stability of multiply charged clusters is also of interest as a test of structure calculations at their higher level [16–20].

In this paper, we present measurements of single, double, triple, and quadruple ionization cross sections of cationic carbon clusters C_n^+ colliding with helium atoms at a fixed velocity $v_p=2.6$ a.u. The size ranges from $n=1$ to $n=10$, extending previous measurements made for $n \leqslant 5$ [21]; the quadruple ionization is also reported. As in [21], the simple independent atom and electron (IAE) model is applied with the purpose of understanding the general behavior of the size-evolution of single and multiple ionization cross sections. It has also been used to predict the internal energies of doubly charged clusters $\{C_n^{2+}\}$ whose stabilities (branching ratios for the nonfragmented part) have been measured. Branching ratios of nonfragmented $\{C_n^{q+}\}$ clusters have been measured in this experiment for $n=3-10$ and $q=2-3$. At variance with fullerenes that have been largely studied [22,23], this constitutes one of the few pieces of experimental information concerning the stability of the small carbon species of charge $q=2,3$ and their evolution with the cluster size. Theoretically, an extensive study within density functional theory (DFT) and coupled cluster single double (triple) [CCSD(T)] formalisms has been recently conducted on small doubly charged carbon clusters [18] and is pursued on triply charged species [20].

The paper is organized as follows: in Sec. II, we present the experimental setup, in particular the technique allowing to identify separately the charge and the mass of each fragment impinging on the detectors. In Sec. III, ionization cross sections are presented and compared to the IAE predictions. In Sec. IV, we present branching ratios for the nonfragmented multiply charged $\{C_n^{q+}\}$ clusters and discuss them in relation with estimated internal energies and existing theories.

II. EXPERIMENTS

The experiments were done at the Tandem accelerator (Institut de Physique Nucléaire, Orsay) with C_n^+ ionic carbon clusters ($n \leqslant 10$) of $2n$ MeV kinetic energy (constant velocity of 2.6 a.u.). Negatively charged clusters C_n^- were produced at the source by sputtering of a graphite rod by keV

TABLE I. Estimated internal energies (IE) of incident C_n^+ clusters at the collision site. Second column: Mean internal energy (and standard deviation of the energy distribution [40]) of C_n^- clusters at the exit of the source (eV); Third column: values of the electron affinity (EA) of C_n clusters [41]; Last column: Mean internal energy (and standard deviation of the energy distribution) of C_n^+ clusters at the collision site.

Cluster size	Internal energies of C_n^- clusters (eV)	EA of C_n clusters (eV)	IE of C_n^+ clusters (eV)
2	0.3 (0.3)	3.3	1.8 (0.5)
3	0.9 (0.5)	2	2.3 (0.7)
4	1.8 (0.7)	3.9	3.2 (0.8)
5	2.7 (0.9)	2.8	3.4 (0.7)
6	3.6 (1)	4.2	4.4 (0.8)
7	4.5 (1.2)	3.3	3.9 (0.7)
8	5.4 (1.3)	4.4	5.0 (0.8)
9	6.3 (1.4)	3.7	4.4 (0.7)
10	7.2 (1.5)	4.5	5.1 (0.7)

C_s^+ ion beam. These species were injected in the Tandem accelerator where they traversed, at the high velocity Terminal, a low pressure gas cell where they lost electrons (stripping). A few million of the clusters became positively charged C_n^+ and were re-accelerated in the second accelerator stage, then magnetically selected towards our experimental setup. Internal energies of species C_n^+ (temperatures) are not precisely known, but may be estimated. The method for extracting the temperature is based on the model of Pargellis *et al.* [24], assuming a thermodynamical equilibrium between the solid (graphite rod) and the gas in which the cluster formation occurs. The fit of our measured C_n^- intensities ($1 \leqslant n \leqslant 9$) with the Pargellis model led to the derivation of a temperature of 3500 K at the cluster source, corresponding to an internal energy of 0.3 (±0.02) eV per vibrational mode for these clusters. In fact, only species having an internal energy below the electron affinity of C_n will survive the few microseconds necessary to reach the stripping site [25], so that internal energies of C_n^- clusters selected in the experiment are lower, especially for high n values (see Table I). To the internal energy of C_n^- clusters one must add the energy acquired in the stripping process. For doing so we assumed that the stripping of the outer electron of C_n^- is done without excitation of C_n, and evaluated the internal energy of C_n^+ resulting from the stripping of an outer or inner valence electron in the neutral cluster. Using ionization energies of valence shell electrons in C_n clusters [26], it turns out that stripping of inner valence electron, depositing more than 10 eV, leads to fragmentation of C_n^+ (lost projectile), whereas stripping of outer valence electron deposits between 1 and 3 eV depending on n. We took for this deposited energy (internal energy of C_n^+ due to the stripping) a mean value of (1.5±0.5) eV whatever n [27]. Final internal energies of C_n^+ clusters at the collision site, whose Gaussian distributions are slightly deformed on the low-energy side, are given in the last column of Table I. The experimental setup [12,28] is schematically presented in Fig. 1; it includes a collision chamber in which a gaseous jet of known profile can be operated [29], an electrostatic deflector separating fragments according to their charge over mass (q/m) ratios, and a detection chamber equipped with eight semiconductor detectors (surfaces ranging between 50 and 600 mm^2) placed suitably in order to intercept all fragments' trajectories. More precisely all neutral, singly, doubly, and triply charged fragments were intercepted, with the exception of triply charged fragments of low size (X_p^{3+}, $p \leqslant 5$) in the case of incident clusters with $n \geqslant 6$. The contribution of the missed triply charged fragments to ionization cross sections was estimated and is negligible. Note that fragments of same charge but different *masses* may impinge on the same detector since the mass is resolved by the detector signal (see below). This explains why the number of used detectors is well below the number of actual trajectories. According to the velocity of the fragments (almost equal to the cluster incident velocity since the velocity change by dissociation is very small) and the distance between the jet and the electrostatic deflector, selection of mass over charge ratios for fragments created between [0–100] nsec after the collision is achieved. In standard operation of these detectors, charge signals are recorded, which provides the total kinetic energy of the fragments hitting the detector, that is, the total mass of the fragments [12]. Recently, we showed that the analysis of the transient currents delivered by the detectors could be used to determine the *number* of fragments hitting the detector and *the mass of each fragment* [30]. This technique has been used for resolving the numerous fragmentation channels of neutral carbon clusters C_n formed by charge transfer [31]. Here, we applied this method to current signals generated by charged fragments as well. This allowed us to distinguish between the impact of a single C_n^{2+} fragment and the impact of two $C_{n/2}^+$ fragments, i.e., to measure branching ratios of non-fragmented C_n^{2+} species for even n values. Branching ratios for all fragmentation channels were also measured in that way and will be published in a forthcoming paper.

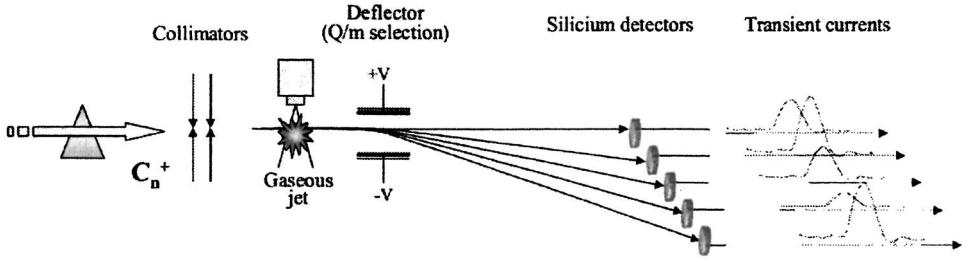

FIG. 1. Schematic view of the experimental setup.

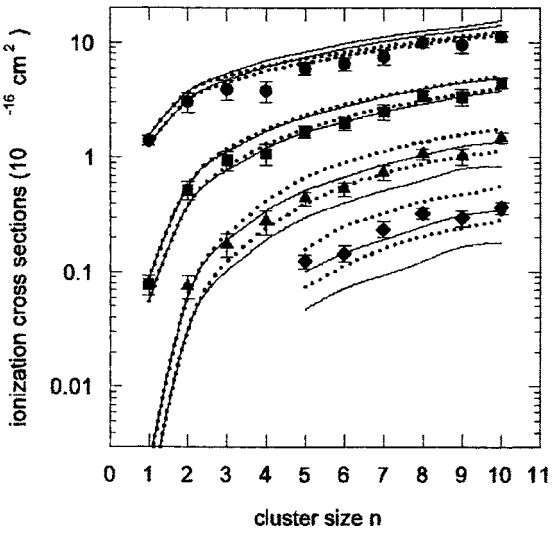

FIG. 2. Measured single (circles), double (squares), triple (triangles), and quadruple (rhombus) ionization cross sections of C_n^+ clusters as a function of n in the collisions of C_n^+ projectiles with helium atoms at a fixed impact velocity (v_p=2.6 a.u.). Solid (dotted) lines are calculated cross sections using the IAE model for linear (cyclic) clusters of lowest energy. The upper and lower curves delimit intervals of theoretical predictions (see text).

III. IONIZATION CROSS SECTIONS

A. Experimental results

In Fig. 2 are reported the experimental cross sections for single (SI), double (DI), triple (TI), and quadruple (QI) ionization cross sections of C_n^+ clusters as a function of n. These cross sections are equal to the total (fragmented and nonfragmented) $\{C_n^{q+}\}$ production cross sections with q =2,3,4,5, respectively. The SI cross sections are roughly proportional to n. By contrast, the increase of DI, TI, and QI cross sections with n is much faster, especially for low n values, as seen in the Fig. 3, where are reported the DI/SI, TI/SI, and QI/SI ratios. In addition to a general increase, these ratios exhibit clear structures which are present on the three curves at the same n values: first an increase with n and a saturation at n=6, then another increase and saturation at n=9, finally a large enhancement at n=10. The existence of these structures has been carefully checked by performing precise evaluation of error bars (which are, for n=5–10, at 95% confidence level). Since ratios are reported, major contributions to error bars of ionization cross sections here disappear (beam intensity, beam-jet overlap). Very small contributions to error bars have been examined and possible systematic errors eliminated: background subtraction, double collisions, and correction due to incomplete mass events. These structures will be discussed, with other results, in connection with predictions of the IAE model in C.

B. Size evolution modeling

We interpret the data within the IAE model [12,21,32,33]. In the model, the C_n^+ cluster is represented by n carbon atoms, one of them being charged (C^+ ion). The atoms are placed at frozen positions during the short collision time

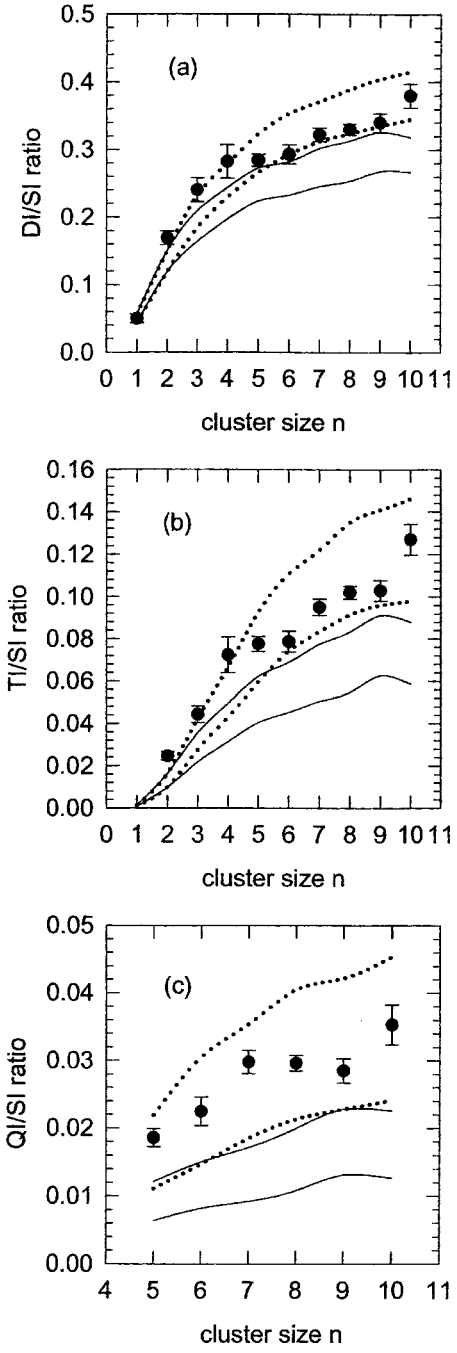

FIG. 3. Same as Fig. 2 but for relative cross sections: DI/SI [Fig. 3(a)], TI/SI [Fig. 3(b)], and QI/SI [Fig. 3(c)].

($t_{\text{coll}} \sim 10^{-16}$ s). Because we showed previously the sensitivity of the IAE predictions to the cluster shape [21] and because various shapes are likely to occur in our experimental beam (see below), calculations for linear as well as cyclic clusters have been performed. The atom's positions were taken from structure calculations performed within DFT-B3LYP and Moeller-Plesset theory (see Table II). For linear clusters, results with the ion charge placed at the center of the cluster and at the terminal of the chain have been averaged. The C_n^+—He collision is treated as $(n-1)$ C→He and one C^+→He independent collisions, occurring at different impact parameters. Ionization cross sections in C_n^+—He

TABLE II. Linear and cyclic isomers of lowest energy for C_n^+ clusters used in the calculations of ionization cross sections. Geometries and total energies have been calculated using the DFT-B3LYP theory for $n \leqslant 8$ [42] and second-order Moeller-Plesset theory for $n=9-10$ [44]. States printed in italics correspond to most stable species. Note that, for C_4^+, coupled cluster calculations [CCSD(T)] predict the cyclic structure to be more stable [21,42,43]. The heights of the transition state between linear and cyclic minima (last column) are extracted from Refs. [43–45], respectively, for $n=4$, $n=5$, and $n \geqslant 6$.

Cluster	Linear isomer L	Cyclic isomer C	Difference between absolute energies (*L*–C) (eV)	Height of the transition state (eV)
C_3^+	$^2\Sigma_u^+$ ($D_{\infty h}$)	*$^2B_2^+$ (C_{2v})*	+0.4	
C_4^+	*$^2\Pi_g$ ($D_{\infty h}$)*	$^2A'$ (C_s)	−0.2	0.9
C_5^+	*$^2\Sigma_u$ ($D_{\infty h}$)*	$^2A_1$ (C_{2v})	−1.6	1.7
C_6^+	*$^2\Pi_u$ ($D_{\infty h}$)*	$^2A_2$ (C_{2v})	−0.4	2.6
C_7^+	$^2\Sigma_g$ ($D_{\infty h}$)	*$^2B_2$ (C_{2v})*	+1.5	2.4
C_8^+	$^2\Pi_g$ ($D_{\infty h}$)	*^2B_u (C_{4h})*	+0.2	
C_9^+	$^2\Sigma^+$ ($D_{\infty h}$)	*$^2A''$ (C_{2v})*	+0.8	4.0
C_{10}^+	$^2\Pi$ ($D_{\infty h}$)	*$^2A'$ (C_{2v})*	+1.9	5.6

collisions only rely on $2s$ and $2p$ ionization probabilities in the $C \rightarrow He$ and $C^+ \rightarrow He$ subsystems. We used probabilities of the form $P_m(b)=N/\lambda^2 P(b/\lambda)$ where $P(b)$ are calculated within the classical trajectory Monte Carlo[1] (CTMC) method, and N, λ are adjustable parameters designed to correct limitations of this theory [21]. The N, λ coefficients, taken similar for the four probabilities [$P_{2s}(b)$, $P_{2p}(b)$ in $C \rightarrow He$ and $P_{2s}(b)$, $P_{2p}(b)$ in $C^+ \rightarrow He$], have been obtained by fitting the theory to the experiment for SI and DI in the $C^+ \rightarrow He$ collision. In the case of DI, a small contribution ($\sim 10\%$), attributed to inner shell $1s$ ionization in C^+ [34], had been subtracted first. Two sets of $\{N,\lambda\}$ values have been considered, depending on whether the fitting was performed on upper experimental values $\{N_1=1.62,\ \lambda_1=1.75\}$ or lower experimental values $\{N_2=1.44,\ \lambda_2=1.75\}$ of SI and DI.[2]

C. Discussion

Results of ionization cross sections within IAE are reported in Figs. 2 and 3 as solid lines for linear clusters and dotted lines for cyclic clusters. Upper curves (lower curves) correspond to IAE predictions with N_1,λ_1 (N_2,λ_2). We see that this uncertainty on N, λ values gives rise to quite large intervals of predictions for ionization cross sections, of the order of ±5% for SI, ±15% for DI, ±25% for TI, and ±40% for QI. However, it is important to remark that it does not affect at all the *comparison* between linear and cyclic clusters since cross sections vary in the same proportion with N,λ. Differences between predictions for linear and cyclic clusters are sizeable, especially at large n. Multiple ionization is theoretically favored for cyclic clusters (see results of TI and QI in Fig. 2) and SI, which is depopulated by multiple ionization, favored for linear clusters. This shape effect is best seen on ionization ratios (see Fig. 3) where in all cases a large increase of ionization ratios is observed with cyclic clusters as compared with linear clusters, an effect magnified when going from DI/SI to TI/SI and to QI/SI [Figs. 3(a)–3(c)].

We now compare with experimental results. Ionization cross sections predicted by the IAE model are in reasonable agreement with the experiment for all theoretical curves, as shown in Fig. 2. This shows that the IAE model is a useful tool for predicting ionization cross sections, in particular multiple ionization cross sections for which, at variance with single ionization, no simple alternative exists (for single ionization, see, for instance, the additivity rule [46]). Another observation, most visible in Fig. 3, is the much better agreement of the model when using cyclic clusters instead of linear clusters in the model. Despite this good agreement, we cannot conclude that the clusters are cyclic. Indeed, the coexistence of various isomers in the beam is probable since internal energies of C_n^+ clusters are always larger—or of the order of—the heights of the transition state between the linear and cyclic isomers of lowest energy (see Tables I and II). We note that a mixture of linear and cyclic clusters (upper curves) would also fit the experiment, on the average.

We now address the question of the structures seen in Fig. 3. Because these structures appear coherently on the three ratios, somehow in a magnified way when going from Figs. 3(a)–3(c), we propose for their interpretation a possible shape effect associated with a change of the *mean* cluster shape. Indeed, a statistical sharing of the C_n^+ internal energy would favor the lowest-energy channel [31], especially when this one is energetically well separated from the other isomers (cases of linear C_5^+, cyclic C_7^+, and cyclic C_{10}^+, for instance, see Table II). This would give rise to changes of percentages between linear and cyclic isomers in the beam as a function of n, which could explain the observed structures, in particular the jumps at $n=7$ and at $n=10$. Nevertheless, further experiments, of a new type, are needed to give a

[1]Note that $2p$ ionization includes direct $2p$ ejection and indirect $2p$ ejection due to autoionizing $2s$ excitation (15% of the direct $2p$ ionization as calculated within CTMC).

[2]Values are different from [21] because new experiments in C^+-He have been performed, leading to slightly larger ($\sim 30\%$) SI and DI cross sections.

TABLE III. Measured branching ratios for nonfragmented C_n^{2+} clusters (second row) and C_n^{3+} clusters (third row) as a function of the cluster size n. In the fourth row are reported the largest values of the height of barrier or dissociation energy ($\max\{HB, E_{diss}\}$) of C_n^{2+}, extracted using Eq. (2) (see text). In the last row are reported calculated dissociation energies of C_n^{2+} clusters performed at the (DFT-B3LYP) level [and CCSD(T) level for the values in parentheses] [18].

n	3	5	6	7	8	9	10
BR (C_n^{2+}) exp. (%)	9.0 (±1.2)	8.3 (±0.4)	10.0 (±1.6)	12.4 (±0.5)	14.4 (±0.8)	17.1 (±1.0)	17.8 (±0.8)
BR (C_n^{3+}) exp. (%)	⋯	⋯	0.12 (±0.02)	0	0	0.15 (±0.02)	1.5 (±0.2)
$\max\{HB, E_{diss}\}$ in C_n^{2+} (eV)	+1.7	+2.7	+3.8	+3.5	+4.6	+4.2	+5
Calculated dissociation energy of C_n^{2+} (eV)	−1.21 (−0.64)	+1.73 (+2.16)	+2.44 (+1.78)	+4.72 (+4.80)	+3.05	+3.51	+5.42

definite answer to this question. In order to test this shape effect in an undoubted way, it appears necessary to work with clusters/ molecules of *known shapes*.[3] Future work will be conducted in that direction.

IV. BRANCHING RATIOS FOR NONFRAGMENTED MULTIPLY CHARGED SPECIES

The branching ratios for nonfragmented C_n^{q+} are given in Table III. These were obtained from experiment as

$$BR(C_n^{q+}) = \frac{C_n^{q+}}{\{C_n^{q+}\}}, \quad (1)$$

where C_n^{q+} is the nonfragmented cluster production and $\{C_n^{q+}\}$ the total production, including both fragmented and nonfragmented contributions.

A striking result is the observation of quite large branching ratios for clusters of large q/n ratios: C_3^{2+}, C_6^{3+}, C_9^{3+}, and C_{10}^{3+}. The case of C_3^{2+} has already been examined. Its unexpected stability (the dissociation energy is negative; see Table III) was already observed in another experiment [36] and theoretically attributed to large and wide barriers (~4 eV) [16]. Unfortunately, calculations of energy barriers are difficult and scarce [16,17]. Calculations on triply charged small carbon clusters are currently under investigation [20].

Another observation is the increase of BR with n, at fixed charge. This effect could be related either to a decrease of the internal energy E^* of C_n^{q+} species with n or, if we assume this internal energy to be constant or to increase with n, to an increase of the height of the barrier (or dissociation energy depending on which one is the largest) with the size. We will show that this is the second situation which can explain the results and that, based on calculations of internal energy of C_n^{2+}, an estimate of the maximum of the height of barrier or dissociation energy in these systems may be derived.

[3]Note that a similar effect, the enhanced multiple ionization for molecules aligned along the ion beam, predicted by IAE [32], was experimentally observed [35].

The internal energy of C_n^{2+} is the sum of the initial energy of C_n^+ (see Table II) and the energy due to ionization E_{ion}. This last quantity has been evaluated within the IAE model in the following way: calculations of single ionization due to ejection of a $2p$ electron, $2s$ electron, or due to single ionization accompanied by electron excitation (SI+E) were performed; results are given in Table IV. The $2p$ ionization was supposed to bring no energy to the C_n^{2+} cluster (ionized atoms created in their ground states) whereas $2s$ ejection was supposed to bring 8.1 or 7.4 eV depending whether ejection occurred from a C or C^+ constituent of the cluster (these values are the differences between the binding energy of the $2s$ electron and the first ionization potential of C and C^+ [37,38]). The energy deposited by {SI+E} has been calculated within IAE by using CTMC predictions for electronic excitation in C and C^+. The minimum value for deposited energy by [SI+E] is 7.2 eV ($2p$-$3s$ transition in C [37] and its mean value was found around 14 eV, almost independent of n [39]. Summing these various contributions, we obtained the E_{ion} values, whose mean values are reported in Table IV.

Now, for prediction of nonfragmented C_n^{++} branching ratios, only the percentage of $2p$ ionization is important since all other processes, bringing in addition to $E^*(C_n^+)$ a minimum of 7.2 eV, will lead to the fragmentation of the doubly charged systems. Supposing that fragmentation occurs if the internal energy $E^*(C_n^{++})$ is just above the largest value of the height of barrier (HB) or dissociation energy (E_{diss}) (i.e., supposing thermodynamical equilibrium) we can show that the branching ratios for nonfragmented C_n^{2+} express exactly as

$$BR(C_n^{2+}) = P_{ion}(2p)P[E^*(C_n^+) \leqslant \max\{HB, E_{diss}\}], \quad (2)$$

where $P_{ion}(2p)$ is the percentage of single ionization into $2p$ and $P[E^*(C_n^+) \leqslant \max\{HB, E_{diss}\}]$ is the percentage of the internal energy distribution of C_n^+ that is below the max of $\{HB, E_{diss}\}$. Since these $E^*(C_n^+)$ distributions are known (cf Sec. II), we can find the values of $\max\{HB, E_{diss}\}$ satisfying relation (2). These values are given in Table III. The obtained values are reasonable, in particular as compared to the calculated heights of barriers of C_3^{++} [16] and dissociation energies of C_n^{2+} (Table III). The size dependence also makes

TABLE IV. Estimated mean energies of C_n^{2+} clusters due to single ionization of C_n^+ species. Calculations were done within the IAE model. In the first and second rows are reported calculated percentages of $2p$ and $2s$ ionization, respectively, with respect to SI. Percentages of single ionization accompanied by excitation $\{SI+E\}$ with respect to SI are given in the third row. Calculations of the mean energies of C_n^{2+} due to single ionization of C_n^+, E_{ion}, obtained by summing the weighted associated energies (see text) are given in the last row.

N	3	5	6	7	8	9	10
P_{ion} $(2p)$ (%)	46	47	47	47	46	46	47
P_{ion} $(2s)$ (%)	42	40	39	38	38	38	37
P $\{SI+E\}$ (%)	12	13	13	15	16	16	16
E_{ion} (eV)	5.6	5.5	5.5	5.8	5.9	5.9	5.9

sense as it is expected that the stability of the species will increase with the size.

V. SUMMARY

In conclusion, we have measured absolute single, double, triple, and quadruple ionization cross sections of C_n^+ clusters in high-energy collisions with helium atoms, at fixed impact velocity (2.6 a.u.) and for n ranging from 1 to 10 ($n=5-10$ for the quadruple ionization). The size evolution of the cross sections has been modelled within the IAE collision model. A good agreement is generally achieved that shows the usefulness of this model, in particular to predict multiple ionization cross sections, which are not easily calculable. Change of mean cluster geometries with the cluster size could be responsible for structures observed on experimental DI/SI, TI/SI, and QI/SI ratios. The study of this shape effect, predicted by the IAE model, will be the subject of future work. Branching ratios for nonfragmented multiply charged clusters were measured in the experiment, providing interesting information on the stability of these species. The observation of triply charged C_6, C_9, and C_{10} clusters demonstrates the robustness of these small systems against Coulomb explosion. Knowing the internal energy of incident C_n^+ clusters and calculating the deposited energy in the ionization process within IAE, we could derive from the measured branching ratios experimental values for the largest of the height of barrier or dissociation energy in C_n^{++} systems. The obtained values are reasonable according to what is known theoretically on these systems. The size dependence also makes sense. This shows that our understanding of the collision process (ionization/excitation and fragmentation) is rather good. The IAE model could then be used in different systems for which experiments are missing or difficult.

ACKNOWLEDGMENTS

The authors thank S. Diaz-Tendero for having provided calculations of the geometries of C_n^+ clusters. They are also indebted to M. Barat and M. Alcami for critical reading of the manuscript.

[1] J. Lequeux and E. Roueff, Phys. Rep. **200**, 241 (1991).
[2] P. Rousselot *et al.*, A & A **368**, 689 (2001).
[3] L. Spitzer and M. Tomasko, Astrophys. J. **152**, 971 (1968).
[4] D. Clayton and L. Jin, Astrophys. J. **451**, 681 (1995).
[5] V. Menella *et al.*, Astrophys. J. **587**, 727 (2003).
[6] M. Barat *et al.*, J. Chem. Phys. **110**, 10758 (1999).
[7] M. Larsen, P. Hvelplund, M. Larsen, and H. Shen, Eur. Phys. J. D **5**, 283 (1999).
[8] R. Ehlich, W. Westerburg, and E. Campbell, J. Chem. Phys. **104**, 1900 (1996).
[9] C. Brechignac *et al.*, Phys. Rev. Lett. **61**, 314 (1988).
[10] T. Lebrun *et al.*, Phys. Rev. Lett. **72**, 3965 (1994).
[11] H. Tsuchida *et al.*, J. Phys. B **31**, 5383 (1998).
[12] K. Wohrer *et al.*, J. Phys. B **29**, L755 (1996).
[13] S. Louc *et al.*, Phys. Rev. A **58**, 3802 (1998).
[14] A. Reinkoster, U. Werner, N. Kabachnik, and H. Lutz, Phys. Rev. A **64**, 023201 (2001).
[15] J. Opitz *et al.*, Phys. Rev. A **62**, 022705 (2002).
[16] H. Hogreve, J. Chem. Phys. **102**, 3281 (1995).
[17] H. Hogreve, J. Mol. Struct.: THEOCHEM **532**, 81 (2000).
[18] S. Diaz-Tendero, F. Martin, and M. Alcami, J. Phys. Chem. A **106**, 10782 (2002).
[19] H. Hogreve and A. Jalbout, J. Chem. Phys. **119**, 8849 (2003).
[20] G. Sanchez, S. Diaz-Tendero, M. Alcami, and F. Martin, Abstracts of the 8th EPS conference on Atomic and Molecular Physics, Rennes 6–10 July (2004).
[21] M. Chabot *et al.*, Eur. Phys. J. D **14**, 5 (2001).
[22] C. Lifshitz, Int. J. Mass. Spectrom. **200**, 423 (2000), and references therein.
[23] E. Campbell and F. Rohmund, Rep. Prog. Phys. **63**, 1061 (2000), and references therein.
[24] A. Pargellis, J. Chem. Phys. **93**, 2099 (1990).
[25] F. Lépine, Ph.D. thesis, Université de Lyon, 2003.
[26] M. Ohno, V. Zakrzewski, J. Ortiz, and W. von Niessen, J. Chem. Phys. **106**, 3258 (1997).
[27] G. Martinet, PhD thesis, Université Paris Sud, 2004.
[28] K. Wohrer *et al.*, J. Phys. B **33**, 4469 (2000).
[29] K. Wohrer, M. Chabot, R. Fossé, and D. Gardès, Rev. Sci. Instrum. **71**, 2025 (2000).
[30] M. Chabot *et al.*, Nucl. Instrum. Methods Phys. Res. B **197**,

155 (2002).
[31] G. Martinet *et al.*, Phys. Rev. Lett. **93**, 063401 (2004).
[32] K. Wohrer and R. L. Watson, Phys. Rev. A **48**, 4784 (1993).
[33] K. Wohrer, M. Chabot, A. Touati, and R. L. Watson, Nucl. Instrum. Methods Phys. Res. B **88**, 174 (1994).
[34] L. Toburen *et al.*, Phys. Rev. A **42**, 5338 (1990).
[35] B. Siegmann *et al.*, Phys. Rev. A **66**, 052701 (2002), and references therein.
[36] A. Kasuya and Y. Nishina, Phys. Rev. B **28**, 6571 (1983).
[37] C. E. Moore, *Atomic Energy Levels NBS* (Nat. Bur. Stand., Dec. 1971).
[38] K. D. Sevier, At. Data Nucl. Data Tables **24**, 344 (1979).
[39] F. Mezdari *et al.* (unpublished).
[40] J. U. Andersen, E. Bonderup, and K. Hansen, J. Chem. Phys. **114**, 6518 (2001).
[41] J. Rienstra-Kiracofe *et al.*, J. Chem. Phys. **102**, 231 (2002).
[42] S. Diaz-Tendero (private communication).
[43] S. Blanksby *et al.*, J. Am. Chem. Soc. **122**, 7105 (2000).
[44] S. Dua and J. Bowie, J. Phys. Chem. A **106**, 1374 (2002).
[45] G. Von Helden, N. Gotts, W. Palke, and M. Bowers, Int. J. Mass. Spectrom. **138**, 33 (1994).
[46] H. Deutsch *et al.* Int. J. Mass. Spectrom. **223–224**, 639 (2003), and references therein.